GIS-Based Estimation of Corrected Standard Penetration Number Using the Best Semi-Variogram Model for Naogaon Sadar

Md. Mahabub Rahman*‡, Md. Nur Alam**, Maharullah Sarder***

* Assistant Professor, Department of Civil Engineering, Faculty of Engineering, Hajee Mohammad Danesh Science and Technology University, Dinajpur-5200, Bangladesh
** Research Scholar, Department of Civil Engineering, Faculty of Engineering, Hajee Mohammad Danesh Science and Technology University, Dinajpur-5200, Bangladesh
*** Research Scholar, Department of Civil Engineering, Faculty of Engineering, Hajee Mohammad Danesh Science and Technology University, Dinajpur-5200, Bangladesh
(mmr.civil@hstu.ac.bd, mdnuralam.hstu.ce@gmail.com, maharul.1807350@std.hstu.ac.bd)

‡Corresponding Author: Md. Mahabub Rahman, Assistant Professor, Department of Civil Engineering, Hajee Mohammad Danesh Science and Technology University, Dinajpur-5200, Bangladesh, Tel: +88 01755881827, mmr.civil@hstu.ac.bd

Received: 12.12.2025 Accepted: 03.04.2026

Abstract - The objective of this study is to calculate the corrected standard penetration number (SPT-Nc) and generate SPT-Nc thematic maps using the best-fitting semi-variogram model. The study is based on 79 standard penetration tests (SPTs) carried out at five SPT measurements per test on each borehole, at depths of 3 m, 6 m, 9 m, 12 m, and ~15 m from the ground surface. A number of factors, such as density, GW table, and overburden pressure, in addition to other correction factors, were introduced to obtain SPT-Nc values. The SPT-Nc at each depth was then computed with Microsoft Excel. Maps obtained as a result of this procedure were subjected to GIS-based thematic maps; for each map a different color was used to indicate the value of SPT-Nc. Maps were generated using ordinary kriging interpolation and tested with six semi-variogram models to find the best-fitting model. Among the six models, the stable, k-bessel and Gaussian semi-variogram models were selected for having the least nugget-to-sill ratio. Since underground consists of clay soil at shallow depths, SPT-Nc was less than 24 and 32 at 3 m and 6 m, respectively. At a depth of 9 m, SPT-Nc ranged from 21 to 35, covering 70.23% of the area measured. At a depth of 12 m, SPT-Nc reached a maximum of 47 due to the decrease in clay content. The greatest values were recorded at 15 m, with 82.6% of the area with SPT-Nc between 38 and 51.

Keywords: GIS; Standard Penetration Number; Semi-Variogram Model; Naogaon Sadar.

1. Introduction

Geotechnical design and stability analysis essentially require accurate information about subsurface conditions that are inherently spatially variable as a result of natural geological processes [1]. Among different in-situ techniques, the standard penetration test is extensively used in engineering practice for its simplicity, inexpensiveness, and empirical correlation with effectiveness parameters of soils [2]. Nonetheless, field standard penetration number (SPT-N) values are affected by various factors such as rod length, hammer energy, type of sampler, diameter of the borehole, and overburden stress [3-4]. In order to alleviate these sources of variation and obtain uniform results across the sites, it is common to correct/adjust the measured field N-values, which yields a standardized or corrected N-value [5].

SPT-Nc data are often analyzed using geostatistical techniques in geographic information systems (GIS) after modifications to demonstrate how soil performance differs. Geo-referenced data may be obtained, stored, analyzed, and presented using a computer system called a GIS. In civil engineering, GIS has been used for several tasks, including liquefaction hazard assessment [6-7], mapping soil distribution and bearing capabilities [8-9], seismic hazard assessment [10-11], land use and land cover change [12], and evaluating the possibility of ground failure [13]. The most frequently used is ordinary kriging, being able to model the spatial dependence effectively by estimating semivariogram [14]. It is important in ordinary kriging to properly select a semivariogram model because it determines how spatial continuity is weakened by

separation distance and thus affects the reliability of kriging estimates. Although deterministic interpolators, such as spline and inverse distance weighting (IDW), are easy to apply and can be used when very few observations of the property exist in the region, typically these do not reflect what is known about the spatial dependence structure and its uncertainty based on soil properties [15]. Of semivariogram models, the Gaussian model is most commonly used in geotechnical problems to produce spatial gradients and a relatively small nugget-to-sill ratio, which means large spatial continuity [16]. This model is found to decrease the estimation error on densely sampled subsurface data and hence enhance interpolation performance [17]. The applicability of the kriging method to the spatial modeling of geotechnical properties have been proved by many researchers [18–20]. For example, Sitharam and Samui used kriging for mapping the subsurface variability in Bangalore based on borehole data [21], whereas Balasubramani and Dodagoudar dealt with anisotropy of soils in Chennai using product-sum covariance models [22]. Vessia et al. applied 3D kriging and geostatistical simulations to estimate borax stockpiles in Turkey, illustrating the benefits of volumetric prediction [23]. Advanced stochastic methods such as sequential Gaussian simulation have been used to quantify the uncertainty and support deterministic mapping [24]. The use of auxiliary covariates in the co-kriging was also reported to increase prediction accuracy [25]. Moreover, anisotropy and stratification have been more comprehensively addressed by directional semivariograms and nested models, allowing the improvement of depth-specific soil property estimation in the heterogeneous subsurface [6, 26–28].

In spite of these progresses, multilayer mapping of SPT-Nc values with correction factors so far is scanty even in the world context and has made no effort in countries like Bangladesh, where geospatial and geostatistical application is relatively new. To fill this gap, this study employs 79 borehole locations in Naogaon Sadar Upazila, Bangladesh, to examine the spatial variation of SPT-Nc at five depths [3 m (10 ft), 6 m (20 ft), 9 m (30 ft), 12 m (40 ft), and 15 m (50 ft)]. The field SPT-N values were adjusted, and a total of six semivariogram models were used to determine the most appropriate model for spatial prediction. The cross-validation, as well as the nugget-to-sill ratios, showed that stable, Gaussian and K-Bessel models best described the data. Finally, ordinary kriging was employed to create thematic depth-wise maps of variation in soil strength, which can be useful for foundation design, land use planning, and urban development.

2. Study Area

The study area is depicted in the northwestern part of Bangladesh (Figure 1). The research area is the Nagaon sadar upazila, one of 11 upazilas in Nagaon District that lies within the Naogaon-5 parliamentary constituency and extends over an area of 275.73 km². It is surrounded by Badalgachhi and Mahadevpur upazilas on the north, Raninagar upazila on the south, Adamdighi (Bogura) and Akkelpur (Joypurhat) upazilas on the east, and Mahadevpur and Manda upazilas on the west. The Little Jamuna and the Tulsi Ganga are the two rivers that flow through the upazila.

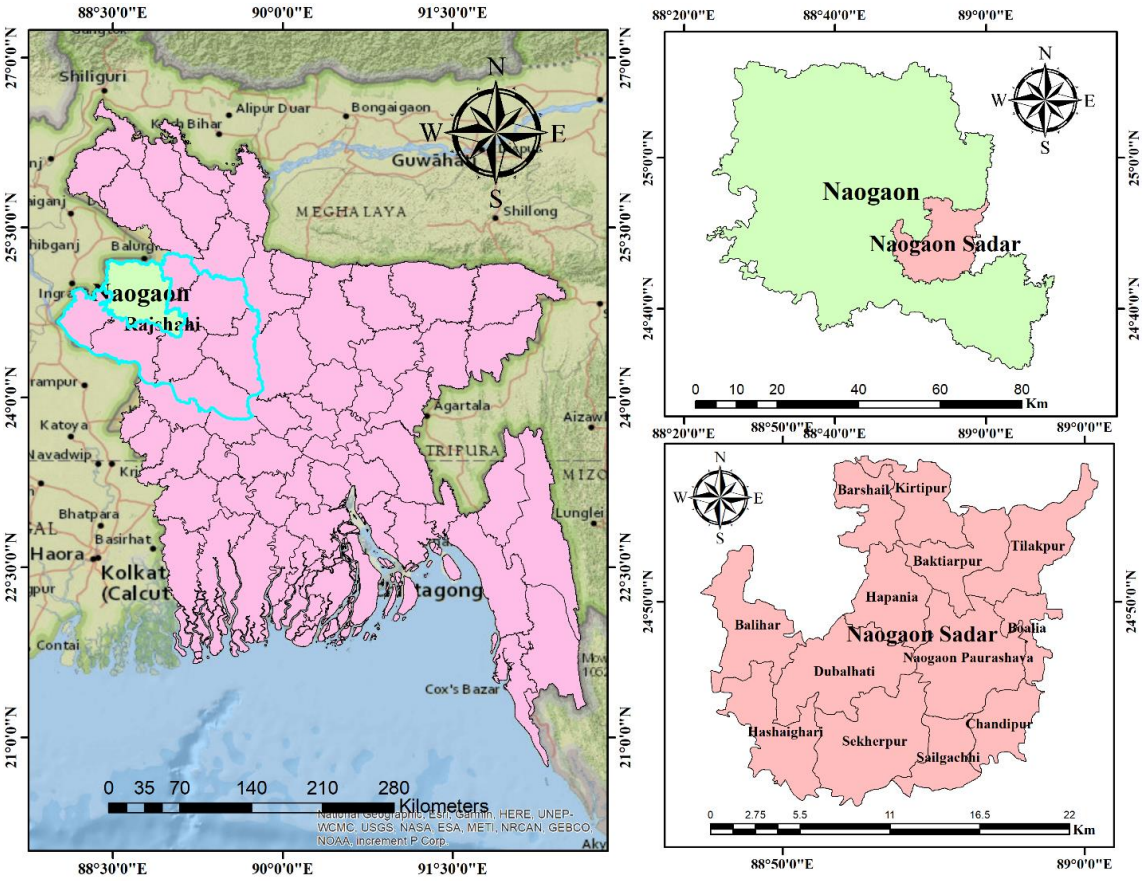

Figure 1. Location of Naogaon sadar.

3. Methodology

3.1 Corrections of SPT-N

The actual SPT-N value is derived from the corrected field N-value that is based on several factors, including conditions of ground water, overburden pressure, and drilling or testing methods. There are many empirical correlations for obtaining the corrected N-value. In the following, we describe in detail the corrected methods.

3.2 SPT-N Corrections for Field Procedures

Field procedure corrections are introduced for penetration hammer energy transfer, sampler geometry and size bore diameter, divided by blow count rate. The energy transfer correction factors accounts for differences in hammer drop height, system efficiency, and the true hammer mass. The sampler correction factor accounts for the area and shape of a sampler, while the borehole correction factor compensates for differences in diameter between boreholes and samplers. In order to account for these procedural effects, Skempton (1986) suggested the correction given by equation 1 [29].

$$N_{(60)} = (N.C_S.C_B.C_R.E_H)/0.60 \quad (1)$$

where, $N_{(60)}$ = corrected N, N = field value; $C_S.C_B.C_R.E_H$ are the sampler, bore dia, rod length, and hammer efficiency correction factor.

The C_S value of Equation (1) is dependent upon the type of sampler's drive used for SPT and one (i.e., C_S =1) shall be chosen when a standard sampler is used. In the SPT field investigations, conventional split spoon samplers were employed in this study. A borehole size correction must be applied for larger boreholes (>12 cm), with the correction factor taken as unity because in the current study we have considered a borehole diameter of 10 cm. As a hand-drop donut hammer was used during field tests, an energy correction factor of 0.6 was applied according to accepted practice [30-32]. In the SPT, energy losses on the drill rods are known to affect its blow count (N), and a rod length correction factor (C_R) is therefore applied in order to have a value more representative for N. Shorter rods also deliver less energy to the sampler because of higher elastic losses, resulting in an underestimation of soil resistance. Therefore, (C_R) can take the value of 0.75 for rod lengths ≤ 4 m; 0.85 for rod lengths ranging between 4 and 6 m; and a unity value when the length of the rod exceeds 10 m since energy transmission losses are minimal [33]. The corrected SPT-N value is obtained after the field N value is multiplied by an appropriate rod length correction factor to maintain uniformity and comparability of test results with tests done at various depths.

3.3 Corrections for Overburden Pressure

The force required to push a testing tool into sandy soil depends upon the overburden pressure of the soil. Near the ground surface, a low pressure is applied, and consequently, less penetration resistance is offered by the same soil (same density), while with increasing depth in the soil body—that is, at higher confining pressure—the same soil resists to a greater degree. With this known, Gibbs and Holtz (1957) recommended using depth-dependent corrections to field SPT-N data [34]. Subsequently, a number of investigators have proposed different correction factors for various depths. The field SPT-N values can be modified to account for the overburden effect by equation 2.

$$N_{1(60)} = C_N \times N_{(60)} \quad (2)$$

Here, C_N is the overburden correction factor. Peck et al. [28], for cn introduced in equation (3) being the well-known form which has already been set up in 1974. As per BNBC (2015) [33], this equation is applicable in Bangladeshi soil also.

$$C_N = 0.77 \times \log(\frac{2000}{\sigma'}) \quad (3)$$

In this work, the σ' is the effective stress in kN/m². At a depth of 3 m approximately, the soil is composed predominantly of silty clay to soft clay having dry unit weight and saturated unit weight equal to 15 kN/m³ and 17 kN/m³ respectively. There is a change in the subsurface soil from silty to sandy ground between 3 and 9 m. Two unit weights for dry and saturated loose sand layers were estimated following the approach proposed in previous studies [30, 35–36] based on equations (4) and (5).

$$\gamma_{moist} = 16 + [0.1 \times N_{(60)}] \quad (4)$$

$$\gamma_{submerged} = 8.8 + [0.01 \times N_{(60)}] \quad (5)$$

3.4 Software

The spatial distribution maps were created with ArcGIS 10.8 by the ordinary kriging interpolation method based on the continuous variations of the measured parameters throughout the study area. Ordinary Kriging, a geostatistical technique that incorporates the regionalized variable theory into the estimation process, was used because of its ability to address spatial correlation as well as local variation and is an unbiased estimator with minimum variance. Sematic variogram analyses were performed on semivariograms of each dataset; the best theoretical model was determined by minimizing cross-validation RMSE and mean error. The modeled semivariogram parameters (nugget, sill, and range) were then used to estimate high-resolution interpolated surfaces. The generated maps successfully emphasize spatial variations and zoning orders and help interpret the subsurface and environmental conditions over the study area more factually [37].

3.5 Semivariogram Model

Spatially continuous surfaces of the measured variables were created using ordinary kriging interpolation due to its strength in considering spatial autocorrelation and minimizing estimation variance. The spatial distribution of the

dataset was examined by empirical semivariograms pre-interpolation, and six theoretical models (spherical, exponential, Gaussian, circular, K-Bessel, and stable) were empirically tested for the best representation of spatial dependence. There are three cross-validation statistics, including RMSE (root mean square error), MSE (mean standardized error), and R^2 (coefficient of determination), to measure the best prediction accuracy. The smallest RMSE and the least close-to-zero MSE model were chosen for fine-tuning interpolation. Then, the adjusted semivariogram parameters (nugget, sill, range) were incorporated in a classical kriging function of ArcGIS to create up-scale spatial distribution maps [36]. This systematic procedure led to reliable interpolation and improved the interpretability of the spatial patterns over the study area.

4. Results and Discussion

4.1 SPT-Nc Modeling

The SPT is the common in situ technique to measure subsurface soil properties. The number of blows required to drive the sampler to a specific depth (usually 30 cm or 12 inches) is referred to as the SPT-N value, which is also known as the 'blow count.' The results are important for geotectonic analysis to understand the density of soil, bearing capacity, etc., which is very helpful and important for designing buildings, slopes, and any other ground structures. SPT-N values are primarily used to assess engineering characteristics of soil and its capacity to bear a load. They are generally considered an important parameter, as they can be field measured, applied over a wide variety of soil types, and possibly strongly correlated to other properties of the soil—SPT-N values are widely used in geotechnical investigations and construction activity. A simplified interpretation of the common values of SPT-N for soil consistency and density is given in Table 1.

Table 1. Density and consistency of soil based on SPT value

SPT-N Value	Soil Consistency (for Clays)	Soil Density (for Sands and Gravels)
0 - 4	Very Soft	Very Loose
5 - 10	Soft	Loose
11 - 20	Medium	Medium Dense
21 - 30	Stiff	Dense
31 - 50	Very Stiff	Very Dense
> 50	Hard	extremely Dens

The following table is a reference to interpret the soil conditions from SPT-N. Utilizing the methods described in the methodology section, the SPT-Nc was calculated based on the field SPT value, and the corrected SPT-N was used to create spatial distribution maps in GIS. Figures 2(a–e) show the spatial distribution of SPT-Nc values at depths of 3, 6, 9, 12, and 15 m, respectively, in the Naogaon district, using the kriging method. Kriging considers spatial autocorrelation and yields continuous transitions between low, medium, and high SPT-Nc zones, capturing the subsurface variability strictly accordingly. This interpolating function enhances the reliability of obtained maps while also rendering them an important instrument for a geotechnical study.

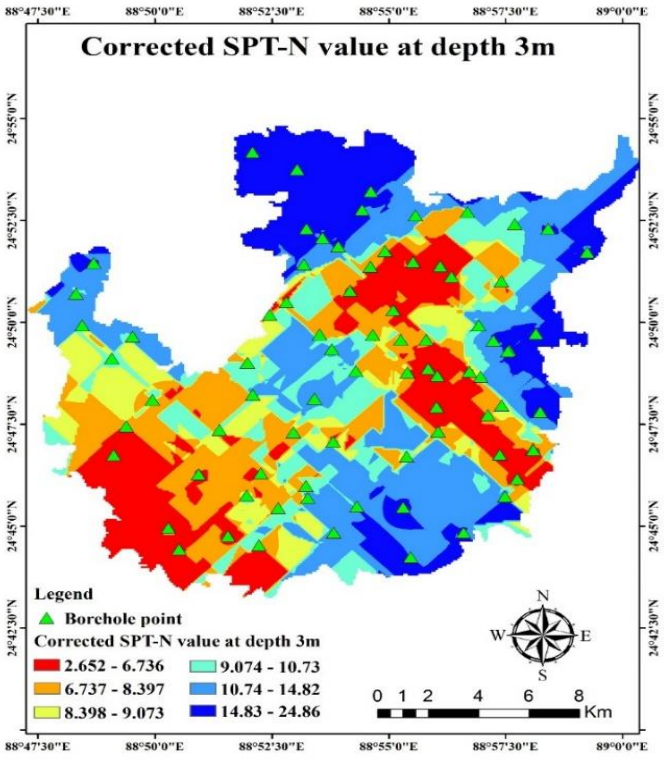

(a)

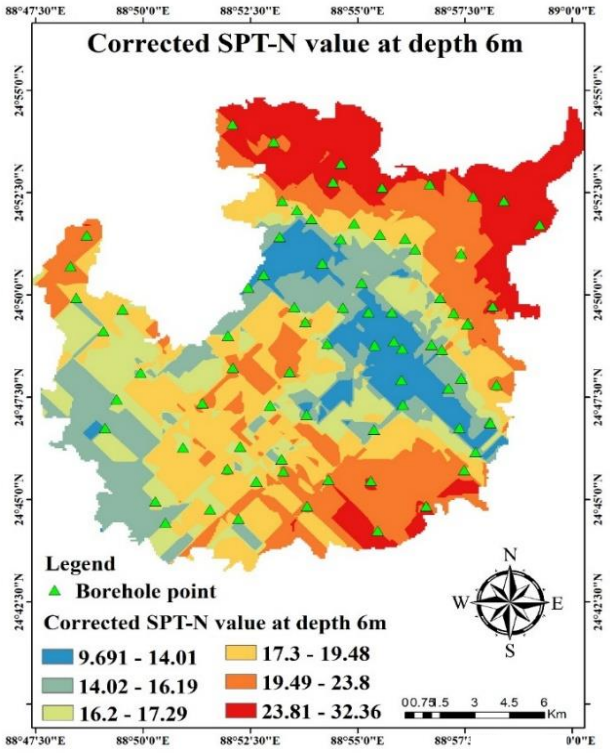

(b)

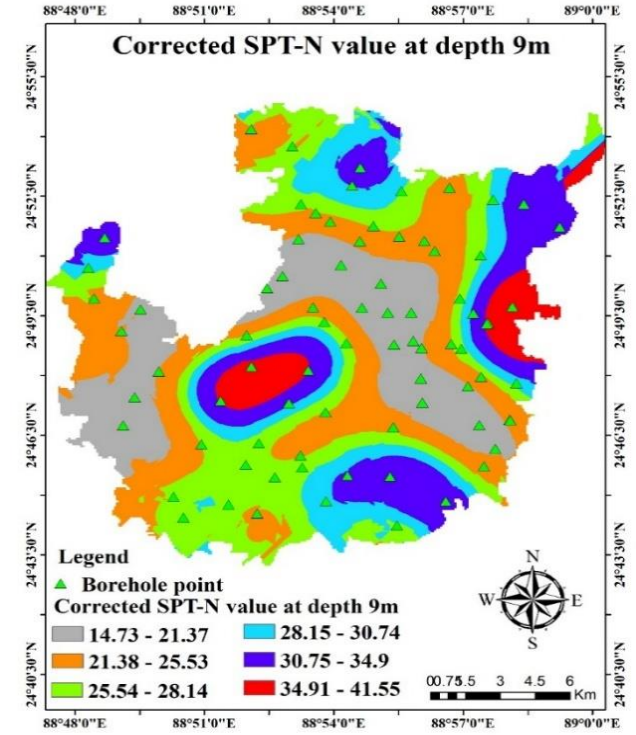

(c)

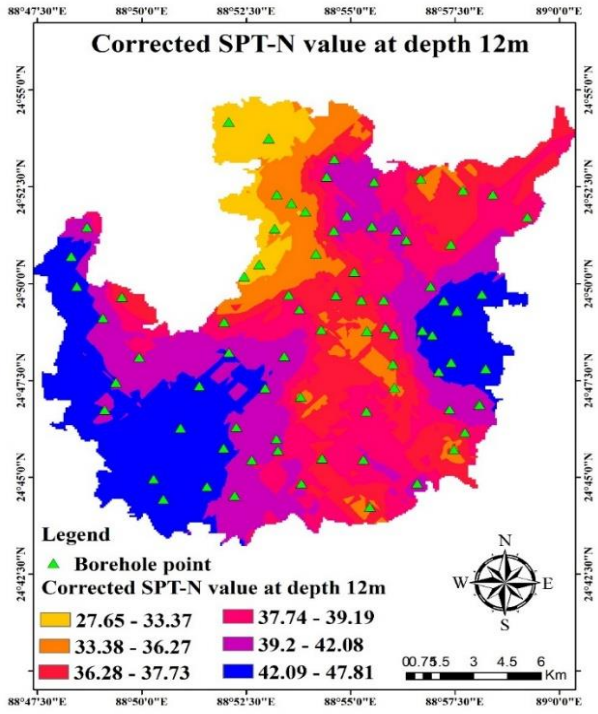

(d)

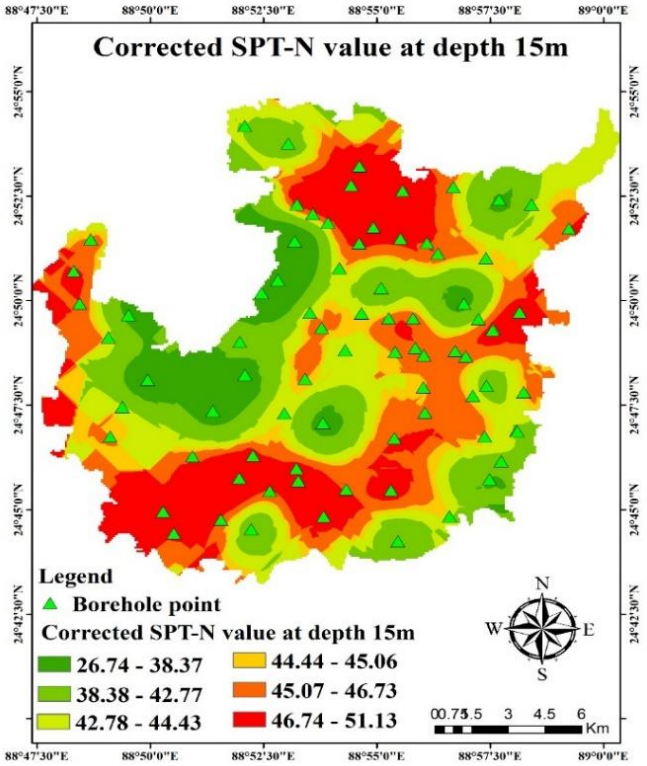

(e)

Figure 2. Variation of SPT-Nc value (a) at 3m depth, (b) at 6m depth, (c) at 9m depth, (d) at 12m depth and (e) at 15m depth.

In particular, at a depth of 3 meters (Figure 2a), the southern and southeastern zones are primarily characterized by low SPT-Nc values (2.65–6.74, orange), which indicate loose soils, while moderate (6.74–14.82, yellow/light blue) and high SPT-Nc values (14.83–24.86) are found in the central and

northern areas, representing medium to dense soils, respectively. At 6 m (Figure 2b), the increase in SPT-Nc is evident, with low-moderate values (9.69–16.19; blue/light green) in the western and southwestern parts of the area, moderate-high values (17.3–23.8; yellow/orange) in a central zone, and very high values (23.81–32.36; red) to the NE, reflecting an overall stiffening behavior as depth increases.

At 9 m depth (Figure 2c), SPT-Nc values range between 14.73 and 41.55, with low values (14.73–21.37, orange) within SW and central-south, intermediate levels (21.38–34.9, yellow/light blue/purple) in central-east regions, and high ones for the central area (34.91–41.55, red), reflecting denser soils on these deposits. At 12 m (Figure 2d), the values range from 27.65 to 47.81, where low (27.65-33.37, orange) is in the northwest and southwest, intermediate (33.38-39.19, yellow/pink) is in the central and east parts, and high (39.2-47.81, purple/blue) is toward the southeast regions, representing the increased level of soil stiffening that has occurred in the soils, while the shear modulus direction's highest increase has also been noticed with time. At 15 m (Figure 2e), SPT-Nc values range from 26.74 to 51.13, with low values (26.74–38.37, green) located in northern, western, and southwestern zones; intermediate ones (38.38–45.06, light green/yellow) found in central and northeastern parts of the study area; and high SPT-Nc values being recorded (45.07–51.13, orange/red) in southern and southeastern sectors of the field. Overall, SPT-Nc increases with depth to represent the densification and settlement of soil, and the most notable stiffening takes place between depths of 12 and 15 m, especially in southern and southeastern zones.

4.2 Semi-variogram Model Evaluation

Figure 3(a) shows a regression of the SPT-Nc with the depth at 3 m, including individual measurements (in red dots) and binned averages (blue crosses). Both the SWRCs have an overall trend given by a regression line; however, these models show considerable scattering when obtaining results at higher distances, showing variation from soil characteristics or measuring conditions. The performance of the model seems to be reasonable with a mean error of −0.327, and small standardized errors. The scatter demonstrates that there are additional factors controlling the results, such as soil type or moisture, and further nonlinearity in modeling could provide better estimations.

This is illustrated in regression (Figure 3b) for a K-Bessel model with 0.00856x + 9.3900, which demonstrates that the dependent increases minimally as distance varies. Fair (mean error 0.323, RMSE 9.61), but a spread decreases the reliability of predictions. Figure 3(c) presents the SPT-Nc histogram at 3 m (79 points, ranging from 0.69 to 3.56 and mean/median of values: 1.88/1.79). The majority of the values range from 0.69 to 2.69, representative of mostly loose or soft soil types with some elevated values in places corresponding to localized denser strata. Moderate dispersion is observed in the distribution (SD 0.974); slightly positive skewedness occurs (0.217); and errors are peaked (kurtosis 1.615), due to generally soft soil conditions punctuated only by some stiffer spots.

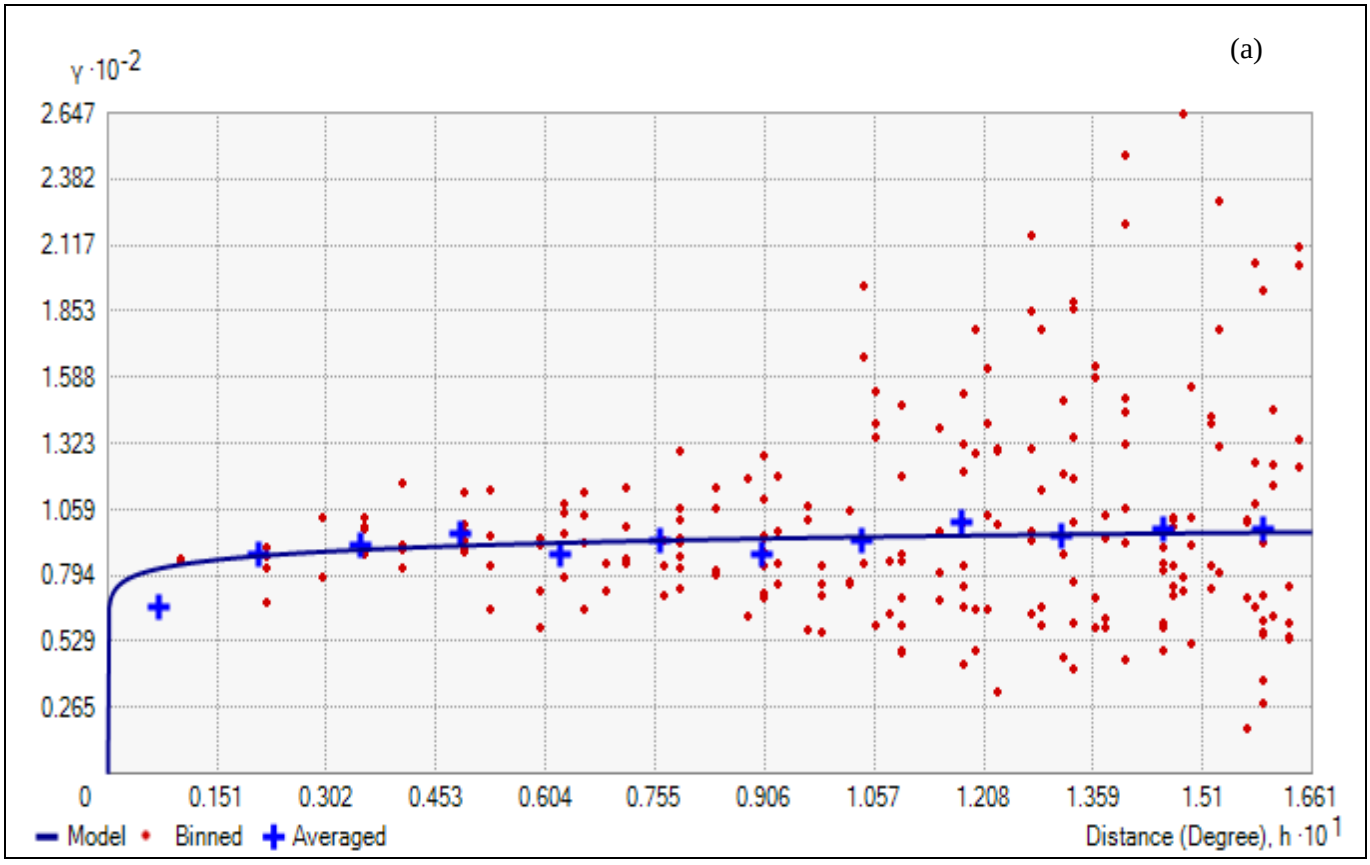

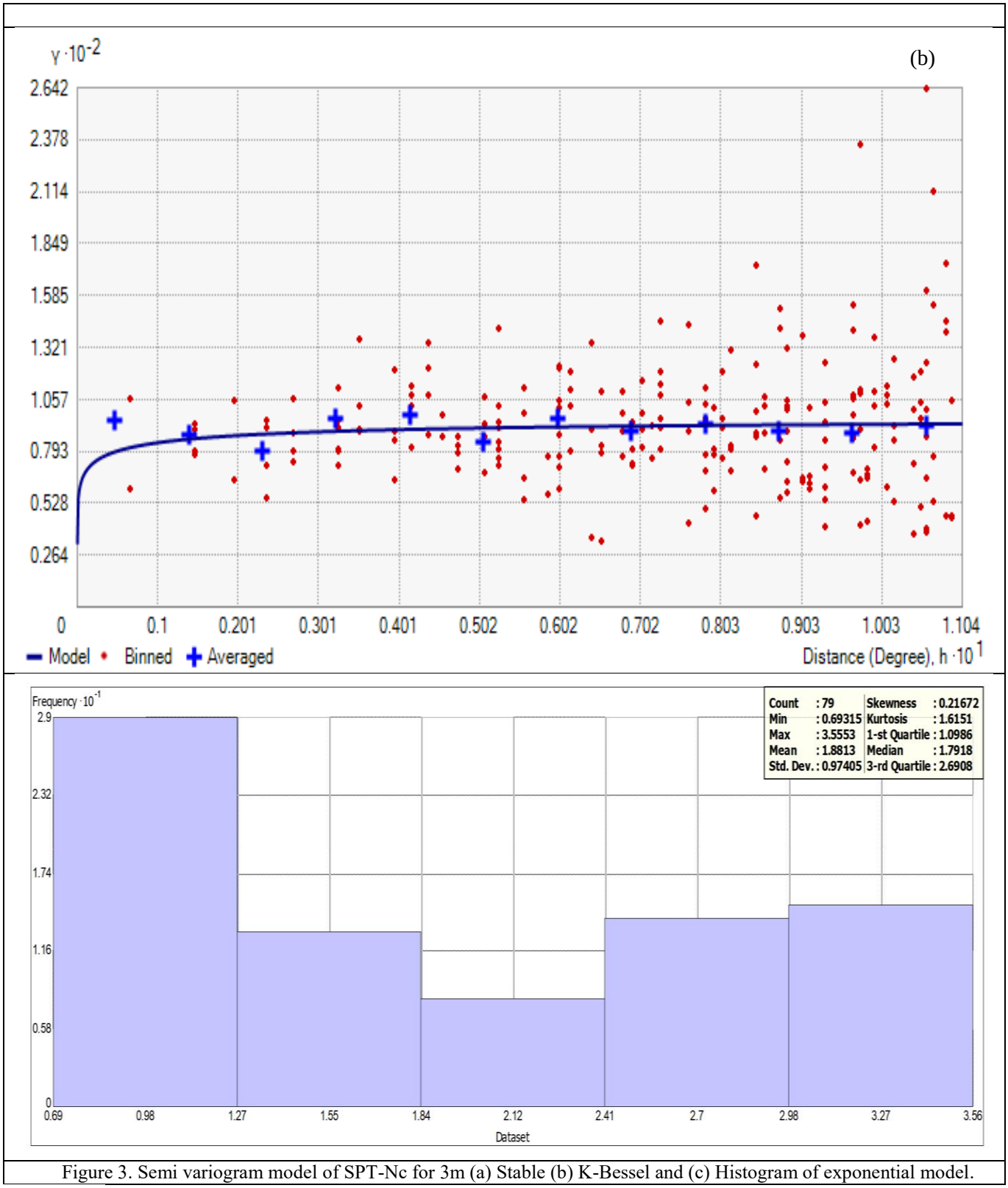

Figure 3. Semi variogram model of SPT-Nc for 3m (a) Stable (b) K-Bessel and (c) Histogram of exponential model.

(c)

Figures 4(a–b) depict regression analysis for SPT-Nc data at a depth of 6 m, and each plot contains measurement points (red filled circles) in addition to binned averages (blue crosses). An RMSE standardized of 0.97063 shows a good fit relative to the standardized range. However, the large spread—especially at larger separations—means that the dependent variable is being modulated by more than distance alone. The almost horizontal trend line also suggests that the impact of distance is really very low at this depth. In order to enhance model prediction, the use of nonlinear emulators and/or additional variables such as soil type and moisture content or environmental factors should be explored. The

higher variation at further distances may justify checking for outliers or irregularities in the measurements. Figure 4(c) shows the histogram of SPT-Nc at 6 m depths for a total of 79 data points, ranging between 1.61 and 3.55. The low standard deviation (0.4868) reflects that most values tightly cluster around the mean (2.80), median (2.71), and a narrow interquartile range (IQR = 2.48–3.21). The distribution is almost symmetrical (skewness − 0.026) and has a mild excess of kurtosis (2.235); it means the distribution is quite peaked. Overweight levels are observed mostly between 2.39 and 2.78, indicating largely compact and dense soils with lower values rarely encountered. Values beyond 3.17 are slightly dangerous, because with a lot of very dense soil, localized zones can occur. From a geotechnical viewpoint, the predominance of increases in SPT-Nc values at this depth indicates that soil strata are characterized by soils with high bearing power and low compressibility and settlement.

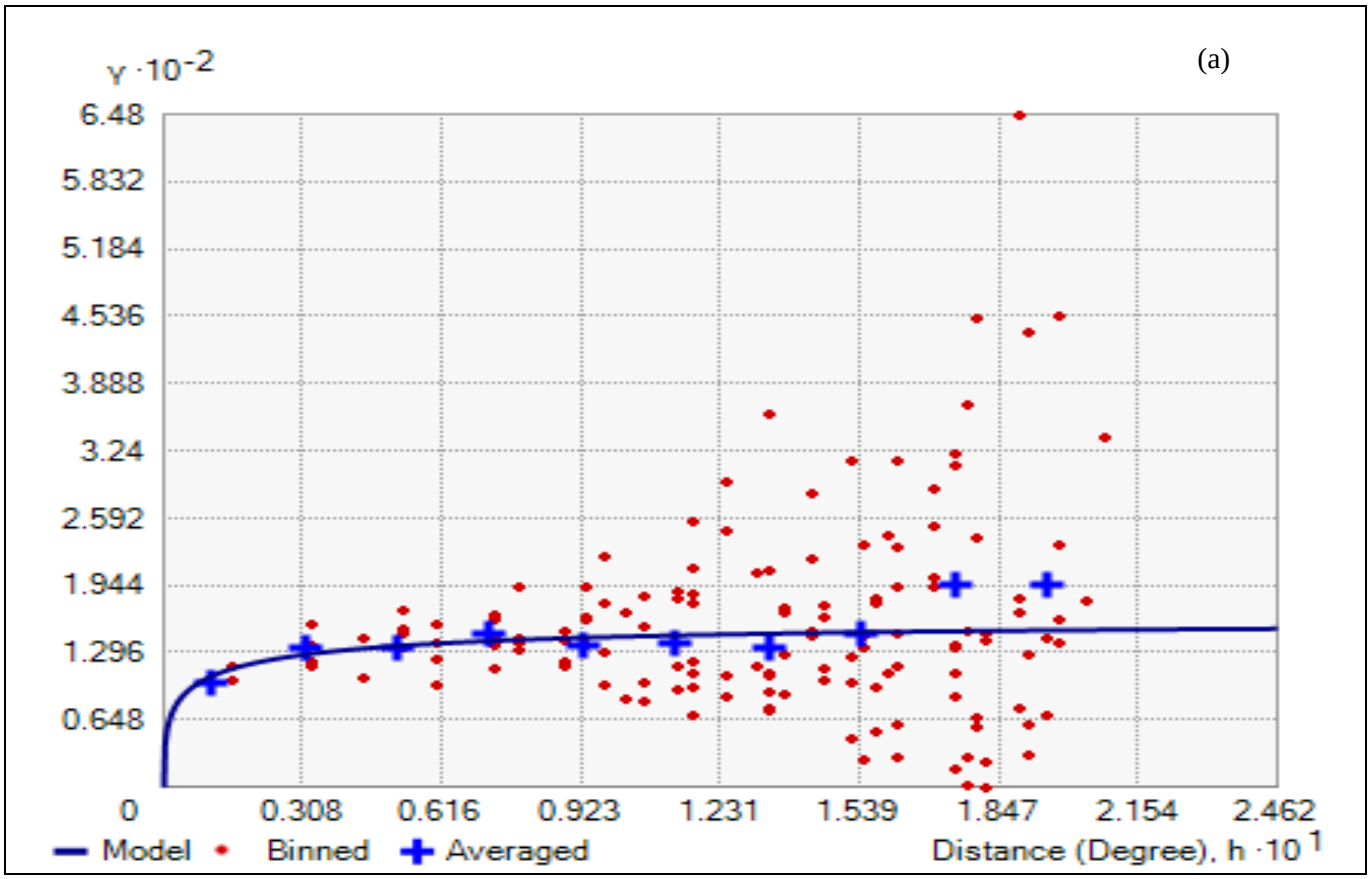

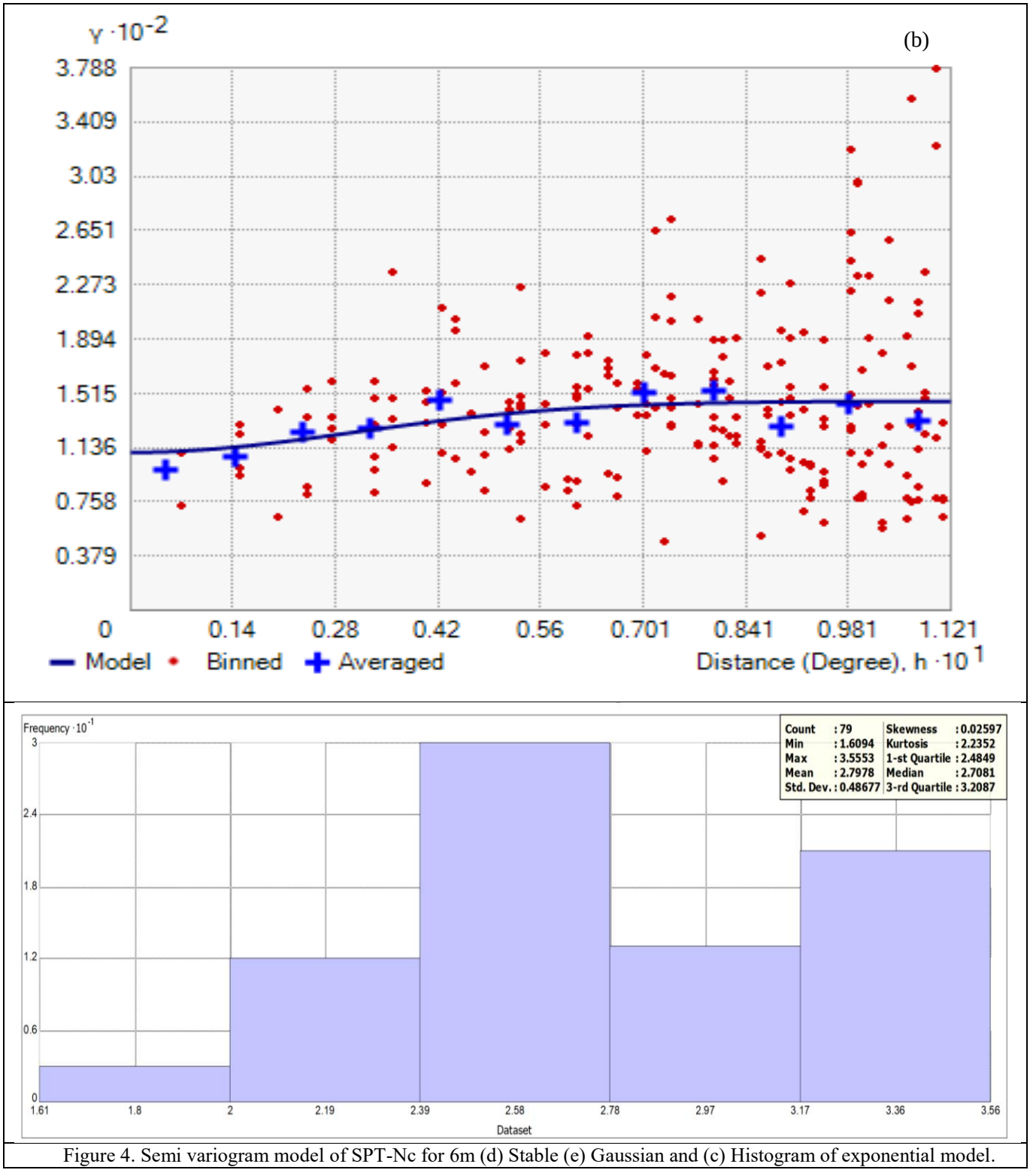

Figure 4. Semi variogram model of SPT-Nc for 6m (d) Stable (e) Gaussian and (c) Histogram of exponential model.

(c)

The relationship between distance and SPT-Nc is presented in Figure 5(a), in which the fitted regression curve (blue) demonstrates a diminishing tendency with the elevation of their distance. The data points reflecting red scattered ones represent a large amount of variability, whereas the blue averaged ones describe the overall trend. The model is acceptable since there was a low overall mean error (–0.2414), a mean standardized error close to zero (–0.0188), and an RMS standardized error near 1 (0.967), although predictability is constrained by the variability in the data. In Figure 5(b), we also demonstrate the similar plot using K-bessel model for a depth of 9m and SPT-Nc shows a little increment by distance (slope = 0.0223). There is significant spread about the best-fit line but the model performs well having mean error close to zero, 0.0468, and a RMS standardized error of 0.970. The trend is well captured by the

model overall, but it is evident that other uncontrolled factors are playing a role. Figure 5(c) Histogram of SPT-Nc values at 9 m depth in 79 samples. Values range between 1.95 and 4.03, with a mean of 3.12 and moderate dispersion (SD = 0.52). It has moderate kurtosis (2.355) and is a little negatively skewed.

The majority of SPT-Nc values are found within the interquartile range (i.e., 2.79–3.49), reflecting mainly compact to dense ground and relatively less of very soft (3.61) zones.

(a)

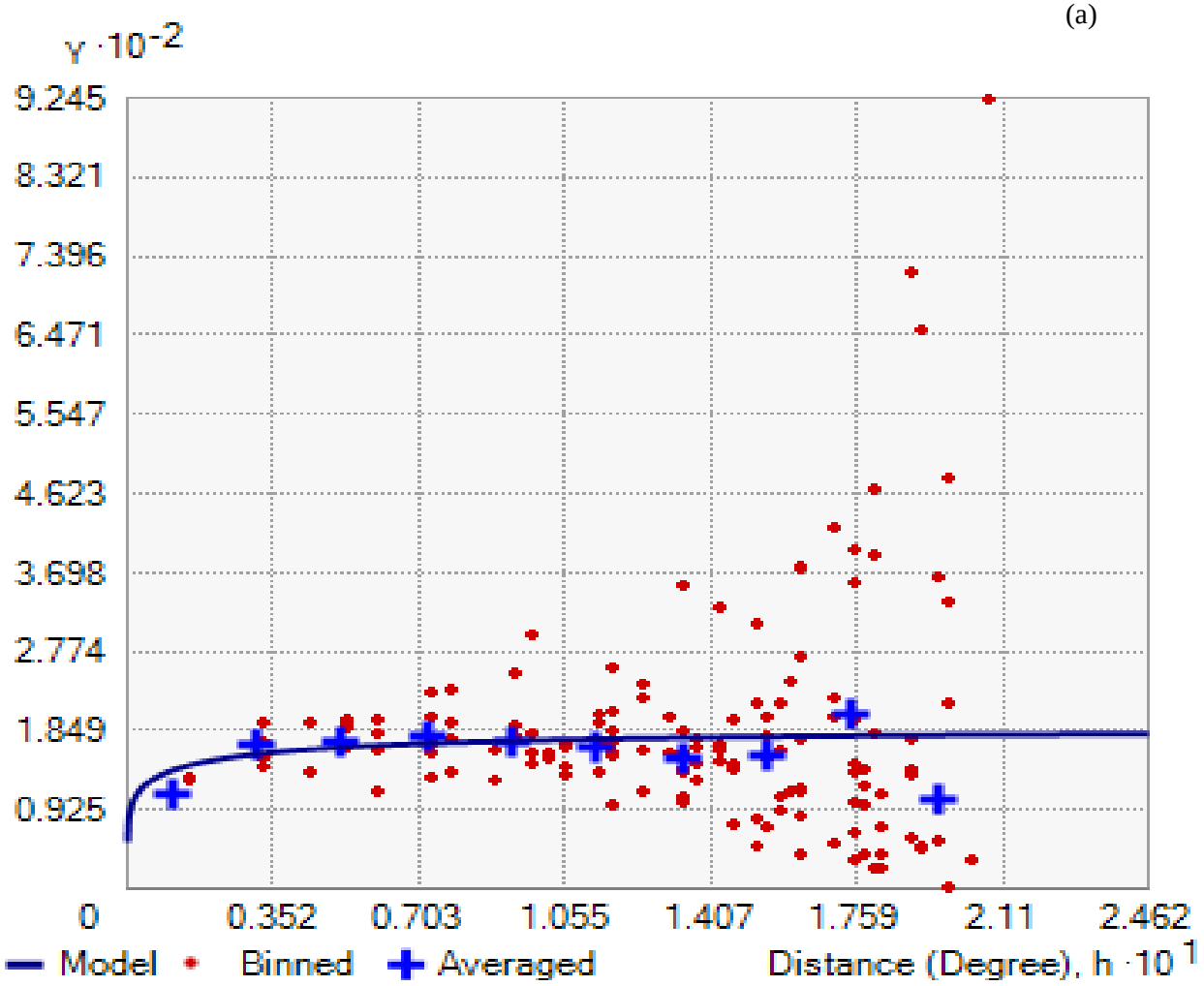

(b)

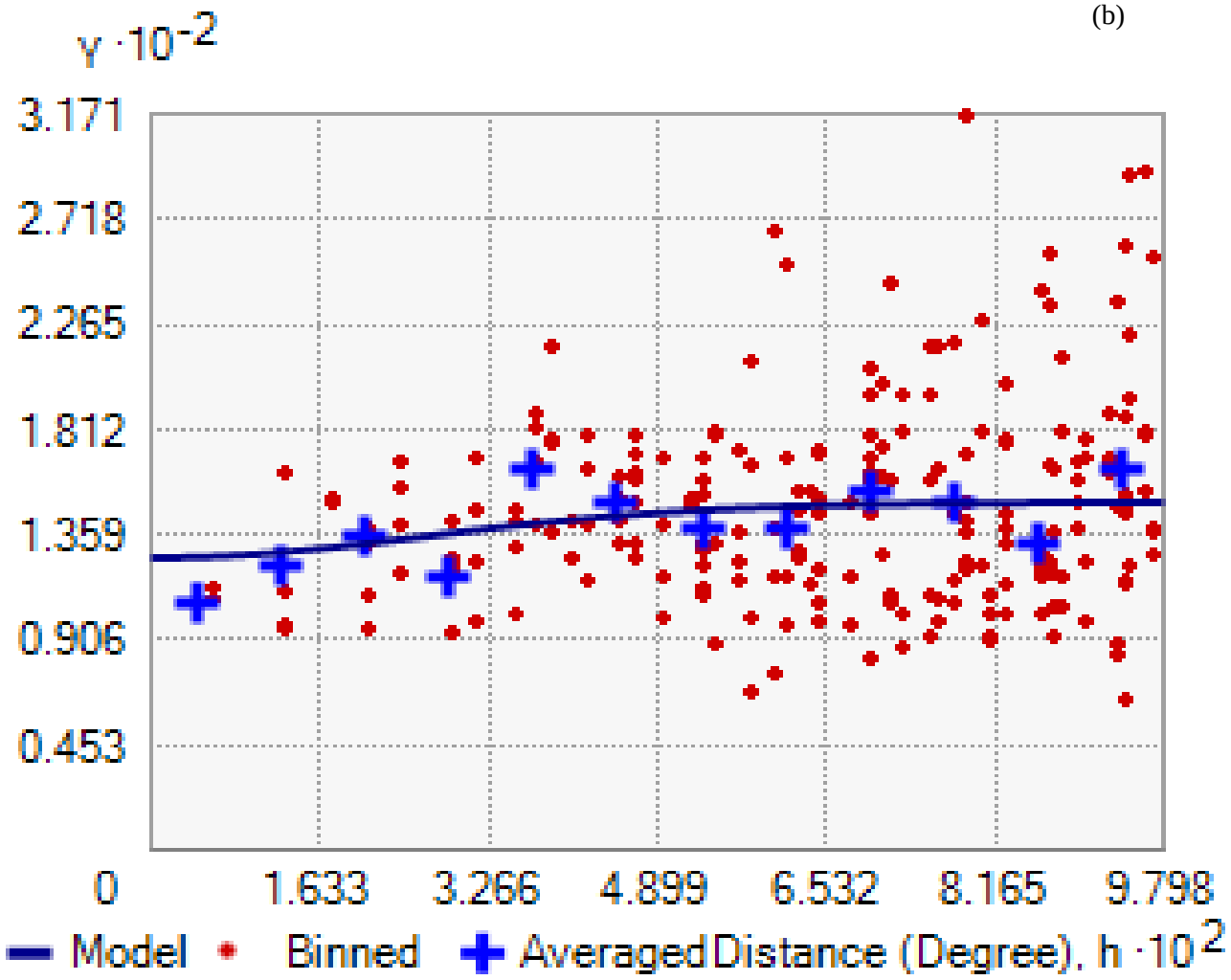

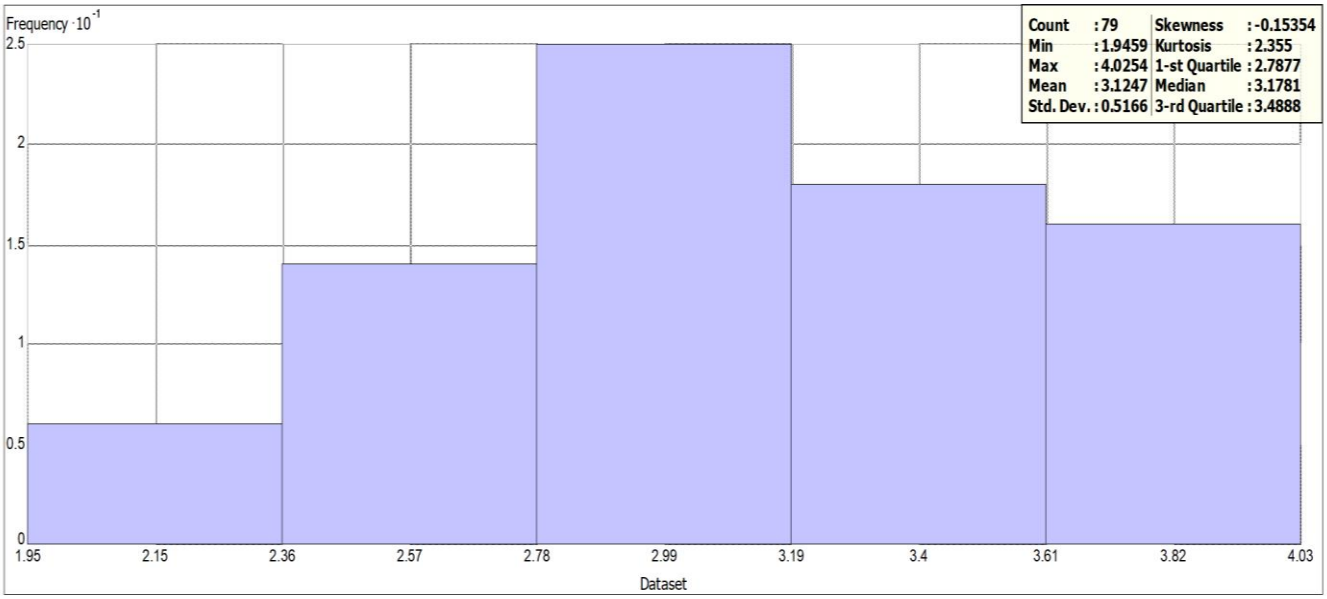

Figure 5. Semi variogram model of SPT-Nc for 9m (a) Stable (b) K-bessel and (c) Histogram of exponential model.

(c)

The distance and the dependent variable at 12 m depth are presented in Figure 6(a). The regression line shows a small positive slope; however, the large scatter of red points indicates there is much happening here. Error measures such as the RMS error and the average standard error are also high, implying that the fit of the model is not very good. The RMS error (0.9827) also indicates that prediction errors are large compared to the data. The blue crosses from the binned points indicate a similar upward trend but also display significant spread. Figure 6(b) shows the histogram of SPT-Nc values at 12 m, which varies between approximately 2.56 and 3.95. Values tend to be concentrated at the upper end (3.67–3.95), with higher soil resistance dominating, and lower readings present in smaller numbers. They are somewhat left-skewed, as suggested by the fact that the mean (3.61) is smaller than the median (3.78). The spread is small (0.37), indicating little variability. With a Q1 and Q3 of approximately 3.34 and 3.91, respectively, an interquartile range (IQR) of around 0.57 shows a well-grouped central distribution pattern. Negatively kurtotic indicates a flatter shape than the normal.

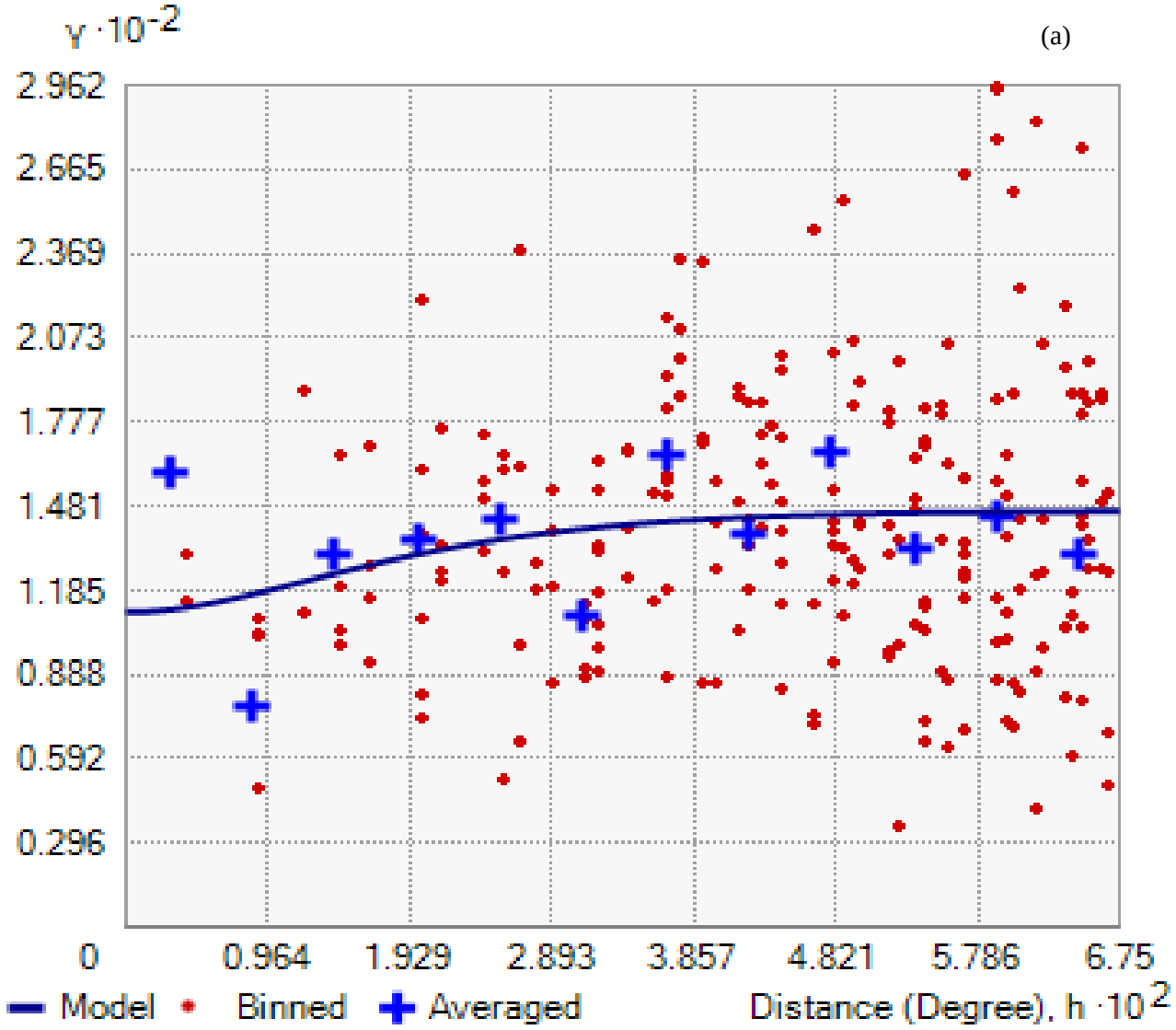

(b)

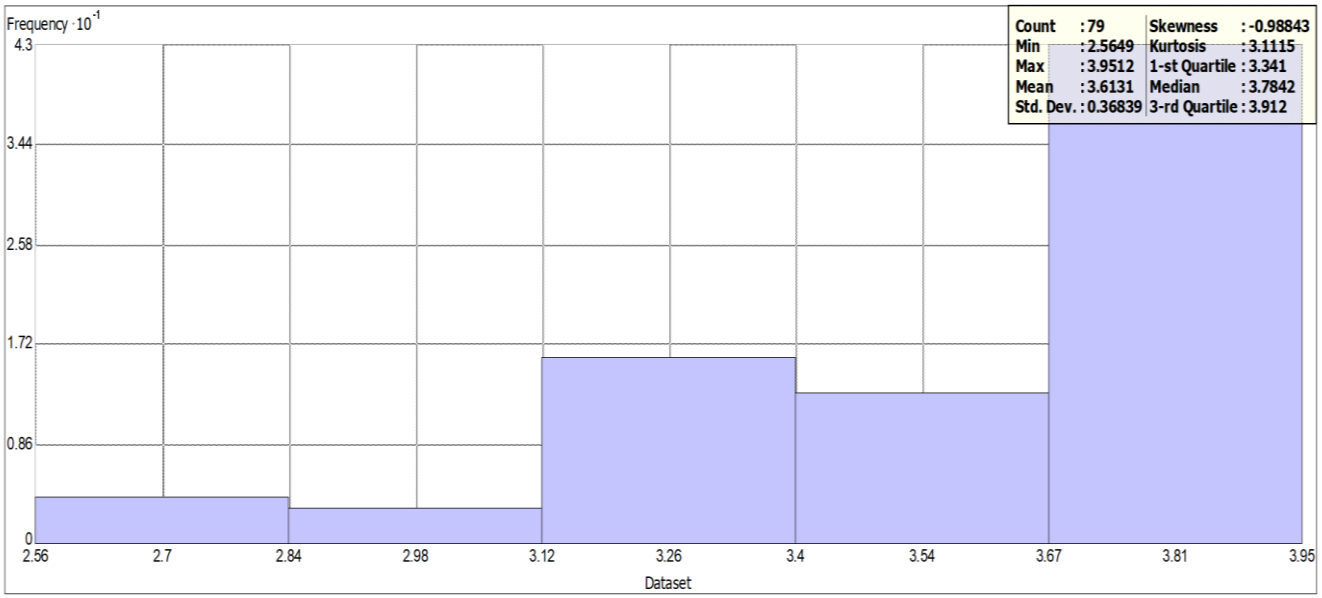

Figure 6. Semi variogram model of SPT-Nc for 12m (a) Stable and (b) Histogram of exponential model.

The regression results at 15 m are displayed in Figure 7(a), where there exists a weak positive correlation between distance and the dependent variable. The data is a little 'all over the place,' making it difficult to really interpret much given that the regression line does not account for the slight positive slope. The RMS error and mean standard errors are less than at 12 m, implying the model provides a relatively better fit. But standardized RMS error demonstrated that there was still a large amount of variability in relation to the data scale. The binned averages tend to approach the line of best fit, highlighting the trend. As a whole, the model does little better at 12 m, and the relationship remains weak with significant variability. In Figure 7(b), the corresponding histogram of SPT values at 15 m depth, which varies approximately from 3.14 to 4.03, is shown. Nearly all of the values are concentrated in the upper interval (3.85–4.03), consistent with little variation of high soil resistance at this depth.

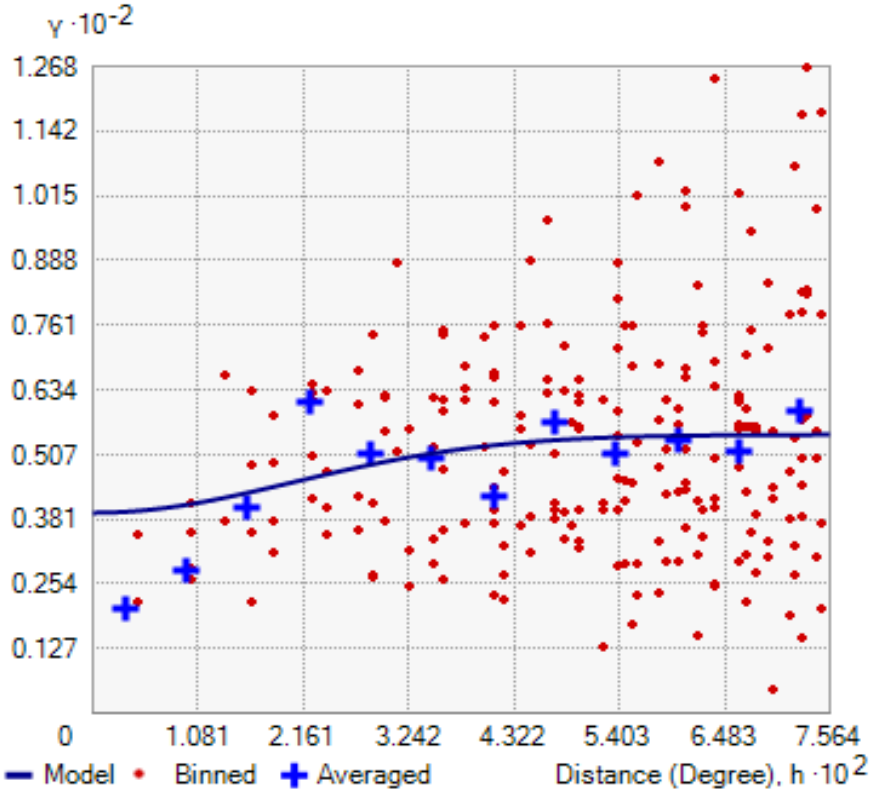

(a)

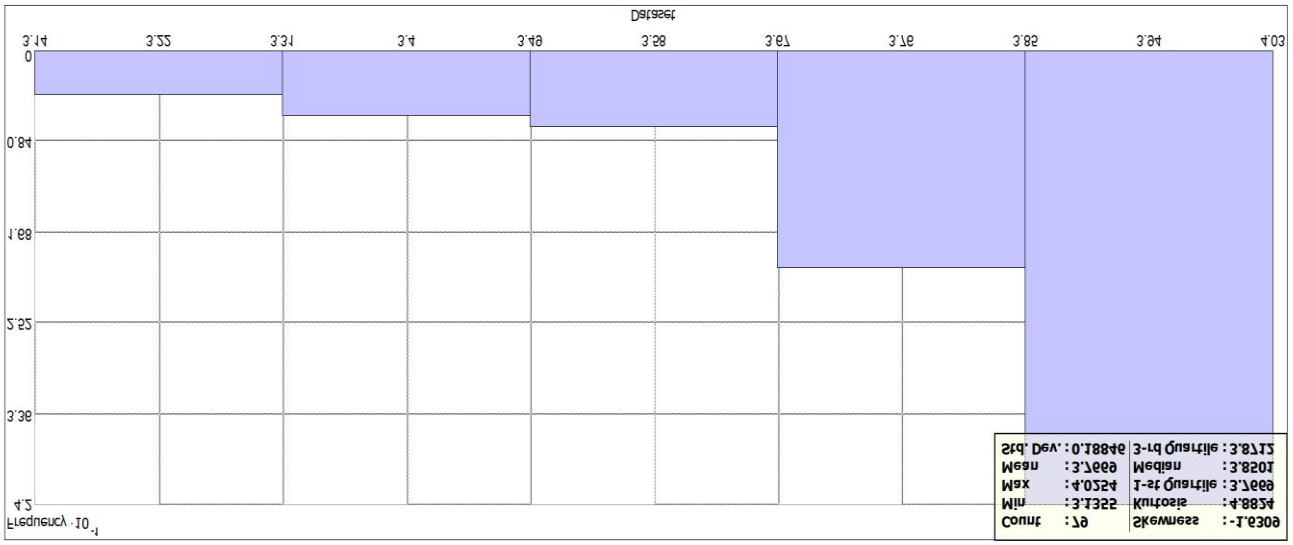

(b) Figure 7. Semi variogram model of SPT-Nc for 15m (a) Stable (b) Histogram of exponential model.

The distribution is highly left-skewed (–1.63) with the mean value of 3.77 and a greater median value of 3.85, respectively. The low SD (0.19) shows the values are tightly clustered. The leptokurtosis is also seen in the data (kurtosis 4.88), with a sharper peak and fatter tails. The interquartile range for the first and third quartiles, 3.77 and 3.87, is very small at about +0.10, which indicates that the central group of data points are tightly packed together with each other.

5. Conclusion

In this study, the corrected SPT-N was calculated using the worldwide applicable empirical equations, and the spatial distribution maps of corrected SPT-N for different depths were prepared based on the best semi-variogram models for the Naogaon Sadar area. A total of 79 borehole sites were studied, where SPT tests were performed every 3 m (0-15 m below ground level). The values of SPT-Nc increase progressively with depth, reflecting a maturation of compaction in all the localities. A progressive compaction trend has been observed in the geotechnical profile. The spatial variability of these values is well captured by Kriging interpolation in GIS, while their distribution and frequency at each depth are shown by histograms. The main results are summarized below:

- ✓ At 3 m depth, high SPT-Nc (14.83–24.86) zones are dominantly located in the northern and northeastern parts. At a depth of 6 m, the high SPT-Nc zones spread, with values ranging from 23.81 to 32.36, indicating a significant increase in soil strength. At 3 m, the stable semivariogram model shows the highest accuracy among the six semivariogram models with a mean error of −0.327 and small standardized errors.
- ✓ Although there is a general increase at 6 m depth, there is substantial variation with space: the northern and northeastern regions have soils that are very dense except for pockets that have relatively low SPT-Nc values in the center. The southern and southwestern areas show much lower (9.691–14.01; loose to medium-dense) SPT-Nc. At 6 m, the Gaussian model gives the best accuracy with a standardized RMSE of 0.97063, which indicates a satisfactory fit relative to the standardized range.
- ✓ High SPT-Nc value points at 9 m are concentrated on the NE and central sites. These compacted areas widen farther south and directly southeast at 12 m and 15 m depths, where stiff soils are most prevalent. At 9m, the stable model has an overall mean error (-0.2414), a mean standardized error close to zero (-0.0188), and an RMS standardized error near 1.
- ✓ Low-resistance southwest and south soils at 9 m shrink to a large extent, indicating better soil conditions with depth.
- ✓ A progressive increase in the minimum and maximum values of SPT-Nc with depth from 9 m to 15 m indicates that naturally consolidated overburdened soil becomes denser and stronger.
- ✓ Similar results can be supported by the histogram patterns: mainly loose soil for 3 m (peak from 0.69 to 0.98), denser soil for 6 m (peak from 2.39 to 2.78), and very dense soil at a depth of about 9 m (peak from 2.78 to 3.19).

Acknowledgements

The authors are very grateful to all individuals associated with this study who have contributed to its completion.

Declaration of Conflicting Interest

The authors declare no conflict of interests.

Nomenclators

Abbreviation	***Description***
SPT-N	*Field standard penetration test number*
SPT-Nc	*Corrected standard penetration test number*
GIS	*Geographic information system*
SD	*Standard deviation*
RMSE	*Root mean square error*
IQR	*Interquartile range*
IDW	*Inverse distance weighted*

References

[1] Baker, R. (1984). Modeling soil variability as a random field. Journal of the International Association for Mathematical Geology, 16(5), 435-448. https://doi.org/10.1007/BF01886325

[2] ASTM D1586. (2011). Standard test method for standard penetration test (SPT) and split-barrel sampling of soils. ASTM International, West Conshohocken, PA.

[3] Decourt, L. (1989). The standard penetration test, state-of-the-art report. Proc. 12th ICSMFE, Rio De Janeiro, 4, 2405-2416.

[4] Liao, S. S., & Whitman, R. V. (1986). Overburden correction factors for SPT in sand. *Journal of geotechnical engineering*, *112*(3), 373-377. https://doi.org/10.1061/(ASCE)0733-9410(1986)112:3(373)

[5] Ghafghazi, M., DeJong, J. T., Sturm, A. P., & Temple, C. E. (2017). Instrumented Becker penetration test. II: iBPT-SPT correlation for characterization and liquefaction assessment of gravelly soils. *Journal of Geotechnical and Geoenvironmental Engineering*, *143*(9), 04017063. https://doi.org/10.1061/(ASCE)GT.1943-5606.0001718

[6] Rahman, M. M., Hossain, M. B., & Roknuzzaman, M. (2023, April). Effect of peak ground acceleration (PGA) on liquefaction behavior of subsoil: A case study of Dinajpur Sadar Upazila, Bangladesh. In *American Institute of Physics Conference Series* (Vol. 2713, No. 1, p. 030002). https://doi.org/10.1063/5.0129770

[7] Hossain, M. B., Roknuzzaman, M., & Rahman, M. M. (2022). Liquefaction potential evaluation by deterministic and probabilistic approaches. *Civil Engineering Journal*, *8*(7), 1459-1481. http://dx.doi.org/10.28991/CEJ-2022-08-07-010

[8] Rahman, M. M., Thakur, S., Ahmed, S. T., & Yasmin, R. (2025). GIS-based development of liquefaction hazard and soil distribution maps for Dinajpur Sadar, Bangladesh. *International Journal of Engineering and Geosciences*, *11*(2), 263-273. https://doi.org/10.26833/ijeg.1662672

[9] Rahman, M. M. (2025). GIS based allowable bearing capacity thematic maps of shallow foundation for Bogura District, Bangladesh. *International Journal of Engineering and Geosciences*, *10*(3), 329-338. https://doi.org/10.26833/ijeg.1589939

[10] Rahman, M. M., & Sarder, M. (2026). GIS-based semi-variogram model selection for the preparation of Modified Mercalli Intensity map of Dinajpur Sadar, Bangladesh. *International Journal of Engineering and Geosciences*, *11*(1), 136-148. https://doi.org/10.26833/ijeg.1656666

[11] Hossain, M. B., & Rahman, M. M. (2025). Seismic microzonation and probability of ground failure assessment caused by liquefaction for Bogura District, Bangladesh. *Journal of Rehabilitation in Civil Engineering*, *13*(2), 222-247. https://doi.org/10.22075/jrce.2024.34111.2086

[12] Rahman, M. M., Nuhash, M. M. R., & Ray, S. (2025, December). Effect of Land Use/land Cover (LULC) Changes on Land Surface Temperature for Chuadanga, Bangladesh. In Proceedings of International Conference on Civil Engineering Research & Innovations (Vol. 12, p. 14).

[13] Rahman, M.M., Hossain, M.B., Islam, M.A., & Rahaman, M.S. (2024). Evaluation of Ground Failure Probability Caused by Soil Liquefaction for Bogura Sadar, Bangladesh. In Proceedings of the 8th International Conference on Civil Engineering for Sustainable Development.

[14] Webster, R., & Oliver, M. A. (2007). *Geostatistics for environmental scientists*. John Wiley & Sons.

[15] Goovaerts, P. (1997). *Geostatistics for natural resources evaluation*. Oxford university press.

[16] Li, J., & Heap, A. D. (2014). Spatial interpolation methods applied in the environmental sciences: A review. *Environmental Modelling & Software*, *53*, 173-189. https://doi.org/10.1016/j.envsoft.2013.12.008

[17] Chen, C., Hu, K., Li, W., Li, Z., & Li, B. (2015). Three-dimensional mapping of clay content in alluvial soils using hygroscopic water content. *Environmental Earth Sciences*, *73*(8), 4339-4346. https://doi.org/10.1007/s12665-014-3720-9

[18] Basarir, H., Kumral, M., Karpuz, C., & Tutluoglu, L. (2010). Geostatistical modeling of spatial variability of SPT data for a borax stockpile site. *Engineering Geology*, *114*(3-4), 154-163. https://doi.org/10.1016/j.enggeo.2010.04.012

[19] Gomez-Hernandez, J. J., & Journel, A. G. (1990, September). Stochastic characterization of grid-block permeabilities: from point values to block tensors. In *ECMOR II-2nd European Conference on the Mathematics of Oil Recovery* (pp. cp-231). European Association of Geoscientists & Engineers. https://doi.org/10.3997/2214-4609.201411102

[20] Hooshmand, A., Delghandi, M., Izadi, A., & Aali, K. A. (2011). Application of kriging and cokriging in spatial estimation of groundwater quality parameters. *African Journal of Agricultural Research*, *6*(14), 3402-3408. https://doi.org/10.5897/AJAR11.027

[21] Sitharam, T. G., & Samui, P. (2007). Geostatistical modelling of spatial and depth variability of SPT data for Bangalore. *Geomechanics and Geoengineering: An International Journal*, *2*(4), 307-316. https://doi.org/10.1080/17486020701678851

[22] Balasubramani, D. P., & Dodagoudar, G. R. (2022). Modelling the spatial variability of Standard Penetration Test data for Chennai City using kriging and product-sum model. *Geomechanics and Geoengineering*, *17*(1), 92-105. https://doi.org/10.1080/17486025.2019.1707884

[23] Vessia, G., Di Curzio, D., & Castrignanò, A. (2020). Modeling 3D soil lithotypes variability through geostatistical data fusion of CPT parameters. *Science of the Total Environment*, *698*, 134340. https://doi.org/10.1016/j.scitotenv.2019.134340

[24] Wang, C. H., Harken, B., Osorio-Murillo, C. A., Zhu, H. H., & Rubin, Y. (2016). Bayesian approach for probabilistic site characterization assimilating borehole experiments and Cone Penetration Tests. *Engineering Geology*, *207*, 1-13. https://doi.org/10.1016/j.enggeo.2016.04.002

[25] Cabalar, A. F., Karabas, B., Mahmutluoglu, B., & Yildiz, O. (2021). An IDW-based GIS application for assessment of geotechnical characterization in Erzincan, Turkey. *Arabian Journal of Geosciences*, *14*(20), 2129. https://doi.org/10.1007/s12517-021-08481-6

[26] Hossain, M. B., & Rahman, M. M. (2025). Seismic microzonation and probability of ground failure assessment caused by liquefaction for Bogura District, Bangladesh. *Journal of Rehabilitation in Civil Engineering*, *13*(2), 222-247. https://doi.org/10.22075/jrce.2024.34111.2086

[27] Skempton, A. W. (1986). Standard penetration test procedures and the effects in sands of overburden pressure, relative density, particle size, ageing and overconsolidation. Geotechnique, 36(3), 425-447. https://doi.org/10.1680/geot.1986.36.3.425.

[28] Peck, R. B., Hanson, W. E., & Thornburn, T. H. (1991). Foundation engineering. John Wiley & Sons.

[29] Skempton, A. W. (1986). Standard penetration test procedures and the effects in sands of overburden pressure, relative density, particle size, ageing and overconsolidation. Geotechnique, 36(3), 425-447. https://doi.org/10.1680/geot.1986.36.3.425

[30] Bolton Seed, H., Tokimatsu, K., Harder, L. F., & Chung, R. M. (1985). Influence of SPT procedures in soil liquefaction resistance evaluations. Journal of geotechnical engineering, 111(12), 1425-1445. https://doi.org/10.1061/(ASCE)07339410(1985)111:12(1425)

[31] Rahman, M. M. (2019). Foundation design using standard penetration test (spt) n-value. Researchgate, 5, 1-39.

[32] Gibbs, H. (1957). Research on determining the density of sands by spoon penetration testing. 4th International Conference on SMFE, 35–39.

[33] BNBC. (2015). Bangladesh National Building Code.

[34] Bowles, J. (1998). Foundation Analysis and Design. McGraw-Hill: New York, NY, USA.

[35] Guo, X. D., Fu, B. J., Ma, K. M., & Chen, L. D. (2001). Utility of semivariogram for spatial variation of soil nutrients and the robust analysis of semivariogram. *Journal of Environmental Sciences (China)*, *13*(4), 453-458.

[36] Silveira, E. M. D. O., Mello, J. M. D., Acerbi, F. W., Reis, A. A. D., Withey, K. D., & Ruiz, L. A. (2017). Characterizing landscape spatial heterogeneity using semivariogram parameters derived from NDVI images. *Cerne*, *23*(4), 413-422. https://doi.org/10.1590/01047760201723042370

[37] Kawser, U., Nath, B., & Hoque, A. (2022). Observing the influences of climatic and environmental variability over soil salinity changes in the Noakhali Coastal Regions of Bangladesh using geospatial and statistical techniques. *Environmental Challenges*, *6*, 100429. https://doi.org/10.1016/j.envc.2021.100429